

# Quantum paramagnets on the honeycomb lattice and field-induced Néel order: Possible application to $\text{Bi}_3\text{Mn}_4\text{O}_{12}(\text{NO}_3)$

R. Ganesh,<sup>1</sup> D. N. Sheng,<sup>2</sup> Young-June Kim,<sup>1</sup> and A. Paramekanti<sup>1,3</sup>

<sup>1</sup>*Department of Physics, University of Toronto, Toronto, Ontario M5S 1A7, Canada*

<sup>2</sup>*Department of Physics and Astronomy, California State University, Northridge, California 91330, USA*

<sup>3</sup>*Canadian Institute for Advanced Research, Toronto, Ontario, M5G 1Z8, Canada*

(Dated: April 22, 2011)

Motivated by recent experiments on the spin-3/2 frustrated bilayer honeycomb antiferromagnet  $\text{Bi}_3\text{Mn}_4\text{O}_{12}(\text{NO}_3)$ , we study the spin- $S$  Heisenberg model on the honeycomb lattice with various additional exchange interactions which frustrate Néel order. Using spin wave theory, exact diagonalization, and bond operator theory, we consider the effects of (i) second-neighbor exchange, (ii) biquadratic exchange for  $S = 3/2$  which leads to an AKLT valence bond solid, and (iii) bilayer coupling which leads to an interlayer dimer solid. We show that the resulting paramagnetic states undergo a transition to Néel order beyond a critical magnetic field. We discuss experimental implications for  $\text{Bi}_3\text{Mn}_4\text{O}_{12}(\text{NO}_3)$ .

The interplay of quantum mechanics and frustrated interactions in quantum magnets leads to a variety of remarkable phases including spin liquid Mott insulators, valence bond crystals, and Bose-Einstein condensates of magnons [1]. Experiments on  $\text{Bi}_3\text{Mn}_4\text{O}_{12}(\text{NO}_3)$  indicate that this material is a possible new candidate for a quantum spin liquid [2]. The octahedral crystal field, together with strong Hund's coupling, leads to Heisenberg-like spin-3/2 moments on the  $\text{Mn}^{4+}$  ions which form a bilayer honeycomb lattice. Despite the bipartite structure, and a large antiferromagnetic Curie-Weiss constant  $\Theta_{CW} \approx -257\text{K}$ , this system shows no magnetic order (or any other phase transition) down to  $T \sim 1\text{K}$  [2]. This observation hints at frustrating interactions which may lead to interesting paramagnetic ground states [3–10].

Recent neutron scattering experiments [11] on powder samples of  $\text{Bi}_3\text{Mn}_4\text{O}_{12}(\text{NO}_3)$  in zero magnetic field indicate that there are short range spin correlations in this material, with some antiferromagnetic coupling between the two layers forming the bilayer, but negligible interactions between adjacent bilayers. Remarkably, a critical magnetic field,  $B_c \sim 6$  Tesla, leads to sharp Bragg spots consistent with three dimensional (3D) Néel order [11]. Motivated by the observation that the field required to induce Néel order appears to extrapolate to a nonzero value at  $T = 0$ , we propose that this system could exhibit a field tuned quantum phase transition into the Néel state. We flesh out this idea by studying various interactions which could frustrate the Néel order in this material.

We first examine the possibility that the Néel order in  $\text{Bi}_3\text{Mn}_4\text{O}_{12}(\text{NO}_3)$  is destroyed by a frustrating second-neighbor exchange ( $J_2$ ) in addition to the dominant nearest neighbor term ( $J_1$ ). Sidestepping the issue of what state results from such quantum melting, we study the magnetic field dependence of the critical  $J_2/J_1$  required to destroy the Néel order. Using spin-wave theory, we show that a nonzero magnetic field enhances the critical  $J_2/J_1$ , opening up a regime where applying a critical field to the non-Néel state yields long-range Néel order.

We next explore other frustrating interactions which might kill Néel order and lead to novel quantum paramagnetic ground states on the honeycomb lattice. We focus here on two valence bond solid (VBS) states, which do not break any symmetries and are expected to show no thermal phase transitions as is the case with  $\text{Bi}_3\text{Mn}_4\text{O}_{12}(\text{NO}_3)$ . (i) Motivated by  $\text{Bi}_3\text{Mn}_4\text{O}_{12}(\text{NO}_3)$ , we study a generalized spin-3/2 model including biquadratic and bicubic spin interactions which permits an Affleck-Kennedy-Lieb-Tasaki (AKLT) ground state [12–14]. Using exact diagonalization (ED) to compute the fidelity susceptibility [15], we show that this model exhibits a direct Néel-AKLT transition. We also obtain the spin gap at the AKLT point. (ii) In view of the fact that  $\text{Bi}_3\text{Mn}_4\text{O}_{12}(\text{NO}_3)$  consists of stacked bilayers, we use a spin- $S$  generalization [16] of the bond operator formalism [17] to show that a sufficiently strong bilayer coupling leads to an interlayer VBS state. Both valence bond solids, the interlayer VBS and the AKLT state, are shown to undergo a magnetic field induced quantum phase transition into a state which exhibits Néel order. Our results on the AKLT state are of broader interest given recent proposals to use this state as a universal quantum computation resource [18].

Finally, we discuss possible experiments on  $\text{Bi}_3\text{Mn}_4\text{O}_{12}(\text{NO}_3)$  which may help to discriminate between the various states we have studied, and to distinguish them from possible  $\text{Z}_2$  spin liquids [9].

*Second-neighbor exchange.*— It has been suggested that the absence of Néel order in  $\text{Bi}_3\text{Mn}_4\text{O}_{12}(\text{NO}_3)$  is linked to non-negligible further neighbor interactions [2]. We therefore study a minimal Hamiltonian,

$$H = J_1 \sum_{\langle ij \rangle} \mathbf{S}_i \cdot \mathbf{S}_j + J_2 \sum_{\langle\langle ij \rangle\rangle} \mathbf{S}_i \cdot \mathbf{S}_j - B \sum_i S_i^z \quad (1)$$

where  $\langle \cdot \rangle$  and  $\langle\langle \cdot \rangle\rangle$  denote nearest and next-nearest neighbor bonds respectively, and  $B$  is a Zeeman field. Let us begin with a classical analysis valid for  $S = \infty$ . When

$J_2=B=0$ , the ground state has collinear Néel order. For  $J_2=0$  and  $B \neq 0$ , the spins in the Néel state start off in the plane perpendicular to the applied field and cant along the field direction until they are fully polarized for  $B > 6J_1S$ . For  $B < 6J_1S$ , the spin components transverse to the magnetic field have staggered Néel order for  $J_2 < J_1/6$ ; this gives way to a one-parameter family of degenerate (canted) spirals for  $J_2 > J_1/6$  [7].

Incorporating quantum fluctuations is likely to lead to melting of Néel order even for  $J_2 < J_1/6$ . Such fluctuations are also likely to completely suppress the classical spiral order [7]. Using spin wave theory, we argue here that a small nonzero  $B$  enhances the stability of the Néel order compared to the zero field case. (i) For small nonzero  $B$ , spin canting leads to a small decrease,  $\propto B^2$ , in the classical staggered magnetization transverse to the field. (ii) On the other hand, one of the two magnon modes (labelled  $\Omega_{\mathbf{k}}^+$ ) acquires a nonzero gap  $\propto B$  at the  $\Gamma$ -point as shown in Fig. 1(a) (for  $S=3/2$  with  $J_2=0.15J_1$  and  $B=0.5J_1S$ ). This suppresses quantum fluctuations. For  $B \ll 6J_1S$ , the latter effect overwhelms the former, leading to enhanced stability of Néel order.

To estimate the ‘melting curve’, we assume that the transverse spin components have Néel order along the  $S_x$ -direction, and use a heuristic Lindemann-like criterion for melting:  $\sqrt{\langle S_x^2 \rangle - \langle S_x \rangle^2} > \alpha \langle S_x \rangle$  where the expectation values are evaluated in linear spin wave theory (see Supplementary Information for details). As shown in Fig. 1(b) and its inset, quantum fluctuations at  $B=0$  lead to melting of Néel order even for  $J_2 < J_1/6$  (i.e., before the classical destruction of Néel order). We set  $\alpha=3$  since this leads to a melting of Néel order for  $S=1/2$  at  $J_2 \approx 0.08J_1$ , in agreement with a recent variational Monte Carlo study by Clark *et al* [9].

For nonzero  $B$ , the ‘melting point’ moves towards larger  $J_2$ , leading to a window of  $J_2$  over which the quantum disordered liquid can undergo a field-induced phase transition to Néel order (see Fig. 1(b)). This is consistent with recent neutron diffraction experiments [11] on  $\text{Bi}_3\text{Mn}_4\text{O}_{12}(\text{NO}_3)$ . The window of  $J_2$  where such physics is operative appears to be small for  $S=3/2$ ; however, disorder effects would suppress the stiffness [19] and may enhance this regime. We expect field induced Néel order even for  $S=1/2$  (see inset to Fig. 1(b)). This can be verified by including a magnetic field in calculations reported in Ref.[9]. Our results also explain recent Monte Carlo simulations of the classical model with  $B \neq 0$  [8]; if  $J_2=0.175J_1$ , as in the simulations, a nonzero  $B$  takes us closer to the melting curve, and may lead to the numerically observed enhanced Néel correlations. Nevertheless, we expect that there will be no field-induced *long-range* Néel order for  $J_2=0.175J_1$  in the classical model.

Next-neighbor exchange thus provides a plausible explanation for the experimental data on  $\text{Bi}_3\text{Mn}_4\text{O}_{12}(\text{NO}_3)$ . We next turn to an exploration of other mechanisms which frustrate Néel order.

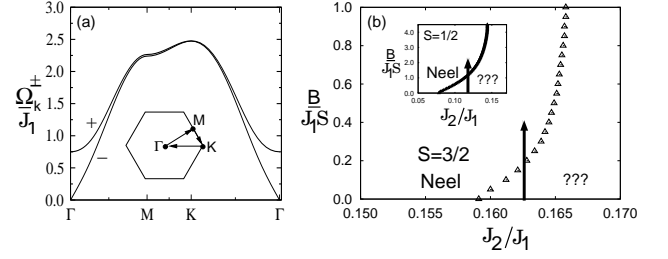


FIG. 1: (a) Dispersion of magnon modes  $\Omega_{\mathbf{k}}^{\pm}$  in the  $J_1$ - $J_2$  model along depicted path in the Brillouin zone for  $J_2=0.15J_1$ ,  $S=3/2$  and  $B=0.5J_1S$ . (b)  $T=0$  melting of Néel order for  $S=3/2$  in the  $B$ - $J_2$  plane (open triangles) obtained using a Lindemann-like criterion,  $\sqrt{\langle S_x^2 \rangle - \langle S_x \rangle^2} = 3\langle S_x \rangle$ . The region “???” is a quantum disordered state - possibly a valence bond solid or a quantum spin liquid. Arrow depicts path along which one obtains a field-induced transition to Néel order. Inset depicts a similar melting curve for  $S=1/2$ .

*AKLT valence bond solid.*— A particularly interesting spin-gapped ground state of a magnet with spin- $S$  atoms on a lattice of coordination number  $z=2S$ , is an AKLT valence bond state. Each spin- $S$  is viewed as being composed of  $2S$  spin-1/2 moments symmetrized on-site, with each spin-1/2 moment forming a singlet with one neighbor [12–14]. It was originally proposed as a realization of Haldane’s prediction of a spin-gapped ground state in 1D integer spin systems [20]. Assuming that the  $\text{Mn}^{4+}$  ions in  $\text{Bi}_3\text{Mn}_4\text{O}_{12}(\text{NO}_3)$  mainly interact with the three neighboring spins in the same plane, this condition is satisfied with  $S=3/2$  and  $z=3$ . The honeycomb lattice AKLT state has exponentially decaying spin correlations [13], and it is the exact, and unique, zero energy ground state of the parent Hamiltonian  $H_{\text{AKLT}} = \sum_{\langle ij \rangle} P_{i,j}^{(3)}$ . Here  $P_{i,j}^{(\ell)}$  denotes a projector on to total spin- $\ell$  for a pair of spins on nearest neighbor sites  $(i, j)$ . Denoting  $T_{i,j} \equiv \mathbf{S}_i \cdot \mathbf{S}_j$ , we find  $P_{i,j}^{(3)} = \frac{11}{128} + \frac{243}{1440} T_{i,j} + \frac{116}{1440} T_{i,j}^2 + \frac{16}{1440} T_{i,j}^3$ . We do not have a microscopic basis, at this point, for such higher order exchange terms in  $\text{Bi}_3\text{Mn}_4\text{O}_{12}(\text{NO}_3)$ ; but it is encouraging to note that the coefficients of such terms are smaller than the leading Heisenberg interaction.

We have investigated, using ED on system sizes  $N=12$ -18, the phase diagram of a generalized spin-3/2 model,

$$H_Q = (1-Q) \sum_{\langle ij \rangle} \mathbf{S}_i \cdot \mathbf{S}_j + gQH_{\text{AKLT}}, \quad (2)$$

which interpolates between a Heisenberg model (at  $Q=0$ ) and  $gH_{\text{AKLT}}$  (at  $Q=1$ ). We set  $g=1440/243$ , so that the coefficient of  $\mathbf{S}_i \cdot \mathbf{S}_j$  is unity. For  $Q=0$ , our analysis of the finite size spectrum shows that the ground state energy  $E_g(N, S^{\text{tot}})$ , as a function of total spin  $S^{\text{tot}}$ , varies as  $S^{\text{tot}}(S^{\text{tot}}+1)$ , in agreement with the expected Anderson tower for a Néel ordered state. It is consistent with earlier work showing Néel order even for spin-1/2 [3, 21, 22]. To establish the Néel-AKLT transition as a function of

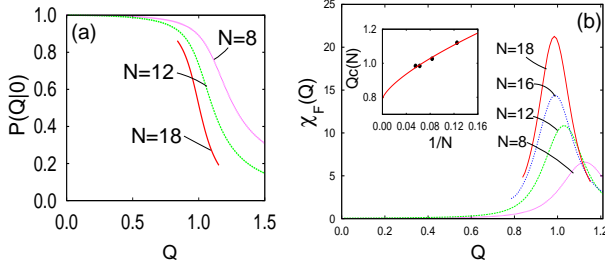


FIG. 2: (Color online) (a) Overlap  $P(Q|0)$  of the ground state at  $Q$  with the Néel state ( $Q=0$ ) for various system sizes  $N$ , showing its rapid drop around the Néel-AKLT transition. (b) Fidelity susceptibility  $\chi_F(Q)$  versus  $Q$  for various system sizes  $N$ , with the peak indicating the Néel-AKLT transition point  $Q_c(N)$ . Inset:  $Q_c(N)$  versus  $1/N$ , together with a fit  $Q_c(N) = Q_c^\infty + bN^{-\frac{1}{2\nu}}$  (with a choice  $\nu \approx 0.7$  assuming an  $O(3)$  quantum phase transition in 2D) which leads to  $Q_c^\infty \approx 0.8$ .

$Q$ , we study overlaps  $P(Q|Q') = |\langle \Psi_g(Q) | \Psi_g(Q') \rangle|$  of the ground state wave functions at  $Q$  and  $Q'$ . As shown in Fig.2(a), the overlap  $P(Q|0)$ , of the ground state wave-function at  $Q$  with the Néel state at  $Q'=0$ , is nearly unity for  $Q \lesssim 0.8$ , suggesting that the ground state in this regime has Néel character. For  $0.8 \lesssim Q < 1.2$ , we observe a dramatic drop of  $P(Q|0)$  for all system sizes, which indicates a Néel-AKLT quantum phase transition. To locate the transition more precisely, we compute the ‘fidelity susceptibility’  $\chi_F(Q) = 2(1 - P(Q|Q+\delta))/\delta^2$ , with  $\delta \rightarrow 0$ , which measures the change of the wavefunction when  $Q \rightarrow Q+\delta$  [15]. Fig.2(b) shows a plot of  $\chi_F(Q)$  (with  $\delta=0.005$ ). We observe a peak in  $\chi_F(Q)$  which indicates a phase transition; this peak shifts and grows sharper with increasing  $N$ . Assuming the thermodynamic transition is at  $Q_c^\infty$ , and that the peak position  $Q_c(N)$  satisfies the scaling relation  $(Q_c(N) - Q_c^\infty) \sim N^{-1/2\nu}$ , with  $\nu \approx 0.7$  for an  $O(3)$  quantum phase transition[23] corresponding to triplon condensation, we estimate the transition point  $Q_c^\infty \approx 0.8$ .

The spin gap  $\Delta_s(N) = E_g(N, S^{\text{tot}}=1) - E_g(N, S^{\text{tot}}=0)$  is plotted in Fig.3(a) for various  $Q$  as a function of  $1/N$ . Assuming a finite size scaling form  $\Delta_s(N) = \Delta_s^\infty + b/N$ , we find a small value for  $\Delta_s^\infty$  for  $Q=0.0, 0.4$ , consistent with a gapless Néel state, while for  $Q=0.9, 1.0$  there appears to be a robust spin gap as  $1/N \rightarrow 0$ . At the AKLT point ( $Q=1$ ), we estimate  $\Delta_s^\infty \approx 0.6$ .

Since the spin gap is finite for  $Q > Q_c$ , we expect that applying a critical field  $B_c \propto \Delta_s$  will lead to a phase transition; the correlation functions of the  $S_z^{\text{tot}}=1$  state at zero field will then reflect the correlations of the ground state for  $B_z > B_c$ . We plot, in Fig.3(b), the spin correlations on two maximally separated sites (for  $N=16$ ) as a function of  $Q$ , and make the following observations. (i) For  $S_z^{\text{tot}}=0$ , the ground state also has  $S^{\text{tot}}=0$ , and  $\langle S_x(i)S_x(j) \rangle = \langle S_z(i)S_z(j) \rangle$  due to spin rotational invariance. At long distance, the spin correlation is strong in the Néel phase, but drops rapidly to small values upon

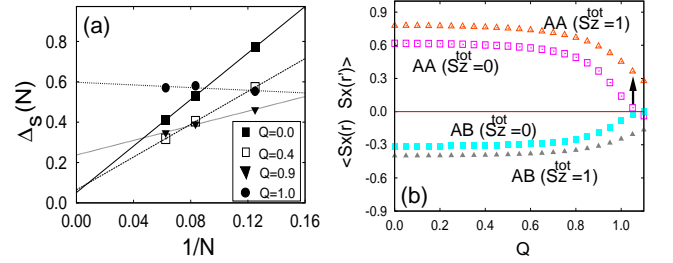


FIG. 3: (Color online) (a) Spin gap,  $\Delta_s(N)$ , versus  $1/N$  for various  $Q$ , with fits to the form  $\Delta_s(N) = \Delta_s^\infty + b/N$ . The small values of  $\Delta_s^\infty$  for  $Q=0.0, 0.4$  are consistent with a gapless Néel state. For  $Q=0.9, 1.0$ , the data are consistent with a robust spin gap  $\Delta_s^\infty$ . (b)  $S_x$ -spin correlations between distant sites on the same (AA) and opposite (AB) sublattices for  $N=16$  system. The spin correlation is Neel-like ( $\pm$ ) for all  $Q$  shown; in the spin gapped AKLT state at  $Q \sim 1$ , it is short ranged and weak in the  $S_z^{\text{tot}}=0$  ground state but it is strongly enhanced (see arrow) in the  $S_z^{\text{tot}}=1$  case.

entering the AKLT state. (ii) In the  $S_z^{\text{tot}}=1$  sector,  $\langle S^z(i)S^z(j) \rangle \neq \langle S_x(i)S_x(j) \rangle$ . Remarkably, in this sector, as opposed to  $S^{\text{tot}}=0$ , we find a strong enhancement of *only* transverse correlations  $\langle S_x(i)S_x(j) \rangle$  between distant sites in the AKLT state; this finite-size result suggests that the AKLT state will undergo, beyond a critical field, a transition into a state with in-plane Néel order.

*Interlayer valence bond solid.* — The Mn sites in a unit cell of  $\text{Bi}_3\text{Mn}_4\text{O}_{12}(\text{NO}_3)$  form an AA stacked bilayer honeycomb lattice. If the interplane antiferromagnetic exchange  $J_c$  is strong compared to the in-plane nearest neighbor exchange  $J_1$ , adjacent spins on the two layers could dimerize and lead to loss of Néel order. To study this interlayer VBS, we begin from the limit  $J_1=0$ ; this leads to the spectrum  $E_j = -J_c(S(S+1) - j(j+1)/2)$ , with  $j=0, 1, \dots, 2S$  denoting the total spin state of the dimer. Restricting attention to the low energy Hilbert space spanned by the singlet and the triplet states, we define generalized spin-S bond operators via:  $|s\rangle = s^\dagger|0\rangle$ , and  $|\alpha\rangle = t_\alpha^\dagger|0\rangle$ , where  $|0\rangle$  is the vacuum, and  $|\alpha(=x, y, z)\rangle$  are related to the  $m_j$  levels of the triplet by  $|z\rangle = |m_j=0\rangle$ ,  $|x\rangle = (|m_j=-1\rangle - |m_j=1\rangle)/\sqrt{2}$ , and  $|y\rangle = i(|m_j=-1\rangle + |m_j=1\rangle)/\sqrt{2}$ . Denoting the two spins constituting the dimer, by  $\mathbf{S}_\ell$ , with layer index  $\ell=0/1$ , we obtain [16]

$$\mathbf{S}_\ell^\alpha \approx (-1)^\ell \sqrt{\frac{S(S+1)}{3}} (s^\dagger t_\alpha + t_\alpha^\dagger s) - \frac{i}{2} \varepsilon_{\alpha\beta\gamma} t_\beta^\dagger t_\gamma, \quad (3)$$

together with the constraint  $s^\dagger s + t_\alpha^\dagger t_\alpha = 1$  at each site.

To treat the effect of  $J_1$ , we use bond operator mean field theory [17] which yields a reasonably accurate phase diagram for the spin-1/2 bilayer square lattice Heisenberg model [23]. Assuming the singlets are condensed in the dimer solid, we replace  $s^\dagger = s = \bar{s}$ , and incorporate a Lagrange multiplier in the Hamiltonian which enforces  $\langle t_\alpha^\dagger t_\alpha \rangle = 1 - \bar{s}^2$  on average. Let  $N$  be the number of spins

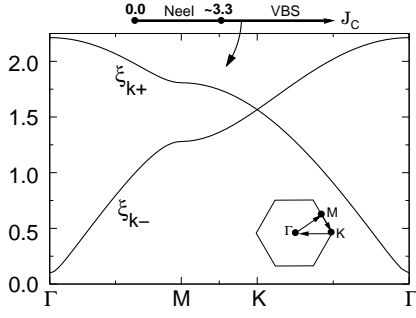


FIG. 4: Phase diagram of the  $S = 3/2$  bilayer honeycomb model obtained using bond operator theory, and triplon dispersion along depicted path in the Brillouin zone within the interlayer VBS state for  $J_c/J_1 = 3.8$  (in units where  $J_1 = 1$ ).

in each honeycomb layer. We then obtain the Hamiltonian  $H = \sum_{\alpha, \mathbf{k} > 0} \Psi_{\mathbf{k}\alpha}^\dagger M_{\mathbf{k}} \Psi_{\mathbf{k}\alpha} + 2NC$ , describing the dynamics of the triplets. Here  $\Psi_{\mathbf{k}\alpha}^\dagger = (t_{\mathbf{k}\alpha 1}^\dagger t_{\mathbf{k}\alpha 2}^\dagger t_{-\mathbf{k}\alpha 1} t_{-\mathbf{k}\alpha 2})$  (with 1, 2 denoting the two sublattices in each layer) and the matrix  $M_{\mathbf{k}}$  takes the form

$$M_{\mathbf{k}} = \begin{pmatrix} A_{\mathbf{k}} & B_{\mathbf{k}} & 0 & B_{\mathbf{k}} \\ B_{\mathbf{k}}^* & A_{\mathbf{k}} & B_{\mathbf{k}}^* & 0 \\ 0 & B_{\mathbf{k}} & A_{\mathbf{k}} & B_{\mathbf{k}} \\ B_{\mathbf{k}}^* & 0 & B_{\mathbf{k}}^* & A_{\mathbf{k}} \end{pmatrix}, \quad (4)$$

with  $A_{\mathbf{k}} = J_c - \mu - J_c S(S+1)$  and  $B_{\mathbf{k}} = \frac{1}{3} \gamma_{\mathbf{k}} J_1 S(S+1) \bar{s}^2$ . Here we have defined  $\gamma_{\mathbf{k}} = 1 + e^{-i\mathbf{k} \cdot \hat{b}} + e^{-i\mathbf{k} \cdot (\hat{a} + \hat{b})}$ , with unit vectors  $\hat{a} = \hat{x}$ ,  $\hat{b} = -\hat{x}/2 + \sqrt{3}\hat{y}/2$ , and the constant  $C = -\frac{\mu}{2}(\bar{s}^2 - 1) - \frac{3}{4}(J_c - \mu - J_c S(S+1)) - \frac{1}{2} J_c \bar{s}^2 S(S+1)$ . Diagonalizing this Hamiltonian leads to the ground state energy per spin  $E_g = \frac{3}{2N} \sum_{\mathbf{k} > 0} (\xi_{\mathbf{k}+} + \xi_{\mathbf{k}-}) + C$  where  $\xi_{\mathbf{k}\pm} = \sqrt{A_{\mathbf{k}}(A_{\mathbf{k}} \pm 2|B_{\mathbf{k}}|)}$ . Setting  $\partial E_g / \partial \bar{s}^2 = \partial E_g / \partial \mu = 0$ , we obtain the mean field values of  $\bar{s}$  and  $\mu$  which minimize the ground state energy subject to the constraint. Solving these equations numerically, we find that the spin- $S$  interlayer VBS is a stable phase for  $J_c > J_*[S]$  where  $J_*[3/2] \approx 3.3J_1$  and  $J_*[1/2] \approx 0.66J_1$ . Quantum Monte Carlo studies of this model would be valuable in firmly establishing the value of  $J_*[S]$  as a function of  $S$ . Fig. 4 shows the triplon dispersion of the  $S = 3/2$  interlayer VBS state at  $J_c = 3.8J_1$  (in units where  $J_1 = 1$ ) along high symmetry cuts in the hexagonal Brillouin zone. For  $J_c < J_*[3/2]$ , or in the presence of a magnetic field which can close the spin gap in the VBS state for  $J_c > J_*[3/2]$ , the low energy triplon mode at the  $\Gamma$ -point condenses; its eigenvector is consistent with Néel order.

**Discussion.**— Motivated by recent experiments on  $\text{Bi}_3\text{Mn}_4\text{O}_{12}(\text{NO}_3)$ , we have studied various honeycomb lattice spin models which support quantum paramagnetic ground states that undergo field-induced phase transitions to Néel order. Detailed NMR studies of isolated nonmagnetic impurities substituted for Mn may help distinguish between these states. The interlayer VBS would have an impurity induced  $S=3/2$  local moment on the

neighboring site in the adjacent layer, the AKLT state would nucleate three  $S=1/2$  moments on neighboring sites in the same plane, while spinless impurities in spin gapped  $Z_2$  fractionalized spin liquids [9], do not generically lead to local moments. Sharp dispersing triplet excitations expected in valence bond solids discussed here could be looked for using single-crystal inelastic neutron scattering; by contrast, a spin liquid may not possess such sharp modes. Specific heat experiments in a magnetic field could test for possible Bose-Einstein condensation of triplet excitations as a route to Néel order.

Finally, dimer crystals with broken symmetry could also be candidate ground states in  $\text{Bi}_3\text{Mn}_4\text{O}_{12}(\text{NO}_3)$  - in which case, disorder must be responsible for wiping out the thermal transition expected of such crystals. If BiMNO does support a valence bond solid ground state, disorder and Dzyaloshinskii-Moriya couplings (permitted by the bilayer structure) may be responsible for the observed nonzero low temperature susceptibility. This is an interesting direction for future research.

We thank J. Alicea, M. Azuma, L. Balents, G. Baskaran, E. Berg, Y. B. Kim, M. Matsuda, and O. Starykh for discussions. This research was supported by the Canadian NSERC (RG,YJ,AP), an Ontario Early Researcher Award (RG,AP), and U.S. NSF grants DMR-0906816 and DMR-0611562 (DNS).

- 
- [1] L. Balents, *Nature* **464**, 199 (2010); R. Moessner and A.P. Ramirez, *Phys. Today* **59**, 24 (2006); T. Giamarchi, Ch. Rüegg, O. Tchernyshyov, *Nat. Phys.* **4**, 198 (2008).
  - [2] O. Smirnova, *et al*, *J. Am. Chem. Soc.*, **131**, 8313 (2009); S. Okubo, *et al*, *J. Phys.: Conf. Ser.* **200**, 022042 (2010).
  - [3] J. B. Fouet, P. Sindzingre, C. Lhuillier, *Eur. Phys. J. B* **20**, 241 (2001).
  - [4] A. Mattsson, P. Fröjdh, and T. Einarson, *Phys. Rev. B* **49**, 3997 (1994).
  - [5] K. Takano, *Phys. Rev. B* **74**, 140402 (2006).
  - [6] Z. Y. Meng, *et al*, *Nature* **464**, 847 (2010).
  - [7] A. Mulder, *et al*, *Phys. Rev. B* **81**, 214419 (2010).
  - [8] S. Okumura, *et al*, arXiv:1004.4441 (unpublished).
  - [9] F. Wang, *Phys. Rev. B* **82**, 024419 (2010); Y.-M. Lu and Y. Ran, arXiv:1007.3266 (unpublished); B. K. Clark, D. A. Abanin, S. L. Sondhi, arXiv:1010.3011 (unpublished).
  - [10] H. Mosadeq, F. Shahbazi, and S. A. Jafari, arXiv:1007.0127 (unpublished).
  - [11] M. Matsuda, *et al*, *Phys. Rev. Lett.* **105**, 187201 (2010).
  - [12] I. Affleck, *et al*, *Phys. Rev. Lett.* **59**, 799 (1987); I. Affleck, *et al*, *Comm. Math. Phys.* **115**, 477 (1988).
  - [13] D. P. Arovas, A. Auerbach, and F. D. M. Haldane, *Phys. Rev. Lett.* **60**, 531 (1988).
  - [14] T. Kennedy, E. H. Lieb, and H. Tasaki, *J. Stat. Phys.* **53**, 383 (1988).
  - [15] A. F. Albuquerque, F. Alet, C. Sire, S. Capponi, *Phys. Rev. B* **81**, 064418 (2010).
  - [16] B. Kumar, *Phys. Rev. B* **82**, 054404 (2010).
  - [17] S. Sachdev and R. N. Bhatt, *Phys. Rev. B* **41**, 9323 (1990).

- [18] J. Cai, A. Miyake, W. Dür, and H. J. Briegel, Phys. Rev. A **82**, 052309 (2010); T.-C. Wei, I. Affleck, R. Raussendorf, arXiv:1009.2840 (unpublished).
- [19] A. Paramekanti, N. Trivedi, and M. Randeria, Phys. Rev. B **57**, 11639 (1998).
- [20] F. D. M. Haldane, Phys. Lett. **93A**, 464 (1983); F. D. M. Haldane Phys. Rev. Lett. **50**, 1153 (1983).
- [21] J. D. Reger, J. A. Riera, and A. P. Young, J. Phys. Cond. Matt. **1**, 1855 (1989).
- [22] Z. Nourbakhsh, *et al*, J. Phys. Soc. Jpn. **78**, 054701 (2009).
- [23] A. W. Sandvik and D. J. Scalapino Phys. Rev. Lett. **72**, 2777 (1994); Y. Matsushita, M. P. Gelfand, and C. Ishii, J. Phys. Soc. Jpn. **68**, 247 (1999).

# Supplementary Material for “Quantum paramagnets on the honeycomb lattice and field-induced Néel order: Possible application to $\text{Bi}_3\text{Mn}_4\text{O}_{12}(\text{NO}_3)$ ”

R. Ganesh,<sup>1</sup> D. N. Sheng,<sup>2</sup> Y. J. Kim,<sup>1</sup> and A. Paramakanti<sup>1,3</sup>

<sup>1</sup>*Department of Physics, University of Toronto, Toronto, Ontario M5S 1A7, Canada*

<sup>2</sup>*Department of Physics and Astronomy, California State University, Northridge, California 91330, USA*

<sup>3</sup>*Canadian Institute for Advanced Research, Toronto, Ontario, M5G 1Z8, Canada*

## SPIN WAVE FLUCTUATIONS AROUND CANTED NÉEL STATE

The Hamiltonian, with a magnetic field and second neighbour exchange, is

$$H = J_1 \sum_{\langle ij \rangle} \mathbf{S}_i \cdot \mathbf{S}_j + J_2 \sum_{\langle\langle ij \rangle\rangle} \mathbf{S}_i \cdot \mathbf{S}_j - B \sum_i S_i^z. \quad (\text{S1})$$

As discussed in the main body, when  $J_2 < J_1/6$  and  $B < 6J_1S$ , Néel ordering is in the plane perpendicular to the magnetic field, but the spins also uniformly cant in the direction of applied field, to maximally gain Zeeman energy. The classical spin state can be characterized by  $\mathbf{S}_r = S(\pm \cos \chi, 0, \sin \chi)$  on the two sublattices. We now define new spin operators, denoted by  $\mathbf{T}_{i,\alpha}$ , via a sublattice-dependent local spin rotation

$$\begin{pmatrix} T_{i,\alpha}^x \\ T_{i,\alpha}^y \\ T_{i,\alpha}^z \end{pmatrix} = \begin{pmatrix} \sin \chi & 0 & (-)^{\alpha+1} \cos \chi \\ 0 & 1 & 0 \\ (-)^\alpha \cos \chi & 0 & \sin \chi \end{pmatrix} \begin{pmatrix} S_{i,\alpha}^x \\ S_{i,\alpha}^y \\ S_{i,\alpha}^z \end{pmatrix} \quad (\text{S2})$$

where  $\alpha = 1, 2$ , is a sublattice index and  $i$  sums over each unit cell.

The ground state has all spins pointing towards the new local- $S^z$  axis. To study spin wave fluctuations, we rewrite the  $T$  operators in terms of Holstein-Primakoff bosons as follows:

$$\begin{aligned} T_{i,\alpha}^z &= S - b_{i,\alpha}^\dagger b_{i,\alpha}, \\ T_{i,\alpha}^x &= \sqrt{\frac{S}{2}}(b_{i,\alpha} + b_{i,\alpha}^\dagger), \\ T_{i,\alpha}^y &= \frac{1}{i}\sqrt{\frac{S}{2}}(b_{i,\alpha} - b_{i,\alpha}^\dagger). \end{aligned}$$

The Hamiltonian can now be rewritten as  $H \approx E_{Cl} + H_{qu}$ . The classical energy  $E_{Cl}$  is proportional to  $S^2$ , and the leading order quantum correction,  $H_{qu}$ , is of order  $S$ . We get the value of the canting angle  $\chi$  by demanding that terms of order  $S^{3/2}$ , which are linear in the boson operators, should vanish, which yields

$$\sin \chi = \frac{B}{6J_1S}. \quad (\text{S3})$$

The classical energy is given by

$$\frac{E_{Cl}}{NS^2} = -\frac{3}{2}J_1 \cos 2\chi + \frac{3}{2}J_2 - \frac{B}{S} \sin \chi. \quad (\text{S4})$$

where  $N$  is the number of sites in the honeycomb lattice. We take the magnetic field  $B$  to be of order  $S$ , so that the Zeeman term  $-BS_i^z$  is treated on the same level as the exchange terms  $J_{ij}\mathbf{S}_i\mathbf{S}_j$ . The leading quantum correction

$$\begin{aligned} \frac{H_{qu}}{SN} &= -\frac{3}{2}J_1 \cos 2\chi + 3J_2 - \frac{B}{2S} \sin \chi \\ &+ \sum_{\mathbf{k} > 0} \psi_{\mathbf{k}}^\dagger H_{\mathbf{k}} \psi_{\mathbf{k}}, \end{aligned} \quad (\text{S5})$$

where

$$\psi_{\mathbf{k}} = \begin{pmatrix} b_{\mathbf{k},1} \\ b_{\mathbf{k},2} \\ b_{-\mathbf{k},1}^\dagger \\ b_{-\mathbf{k},2}^\dagger \end{pmatrix}; H_{\mathbf{k}} = \begin{pmatrix} I_{\mathbf{k}} & F_{\mathbf{k}} & 0 & G_{\mathbf{k}} \\ F_{\mathbf{k}}^* & I_{\mathbf{k}} & G_{\mathbf{k}}^* & 0 \\ 0 & G_{\mathbf{k}} & I_{\mathbf{k}} & F_{\mathbf{k}} \\ G_{\mathbf{k}}^* & 0 & F_{\mathbf{k}}^* & I_{\mathbf{k}} \end{pmatrix} \quad (\text{S6})$$

with

$$\begin{aligned} I_{\mathbf{k}} &= 3J_1 \cos 2\chi - 6J_2, \\ &+ 2J_2\{\cos k_a + \cos k_b + \cos(k_a + k_b)\} + \frac{B}{S} \sin \chi, \\ F_{\mathbf{k}} &= J_1 \gamma_{\mathbf{k}} \sin^2 \chi \equiv |F_{\mathbf{k}}| e^{i\eta_{\mathbf{k}}}, \\ G_{\mathbf{k}} &= -J_1 \gamma_{\mathbf{k}} \cos^2 \chi, \end{aligned}$$

where  $\gamma_{\mathbf{k}}$  is as defined in the main body. This Hamiltonian can be diagonalized by a bosonic Bogoliubov transformation. The eigenvalues are given by

$$\Omega_{\mathbf{k}}^\pm = \sqrt{(I_{\mathbf{k}} \pm |F_{\mathbf{k}}|)^2 - |G_{\mathbf{k}}|^2}. \quad (\text{S7})$$

The transformation matrix is given by

$$P = \begin{pmatrix} U_{2 \times 2} & 0 \\ 0 & U_{2 \times 2} \end{pmatrix} \begin{pmatrix} C_{2 \times 2} & S_{2 \times 2} \\ S_{2 \times 2} & C_{2 \times 2} \end{pmatrix},$$

where

$$U_{2 \times 2} = \frac{1}{\sqrt{2}} \begin{pmatrix} -e^{i\eta_{\mathbf{k}}} & e^{i\eta_{\mathbf{k}}} \\ 1 & 1 \end{pmatrix}; \quad (\text{S8})$$

$$C_{2 \times 2} = \begin{pmatrix} \cosh \theta & 0 \\ 0 & \cosh \phi \end{pmatrix}; S_{2 \times 2} = \begin{pmatrix} \sinh \theta & 0 \\ 0 & \sinh \phi \end{pmatrix}, \quad (\text{S9})$$

where the angles  $\theta$  and  $\phi$  are given by

$$\begin{aligned} \tanh 2\theta &= \frac{|G_{\mathbf{k}}|}{I_{\mathbf{k}} - |F_{\mathbf{k}}|}, \\ \tanh 2\phi &= \frac{-|G_{\mathbf{k}}|}{I_{\mathbf{k}} + |F_{\mathbf{k}}|}. \end{aligned} \quad (\text{S10})$$

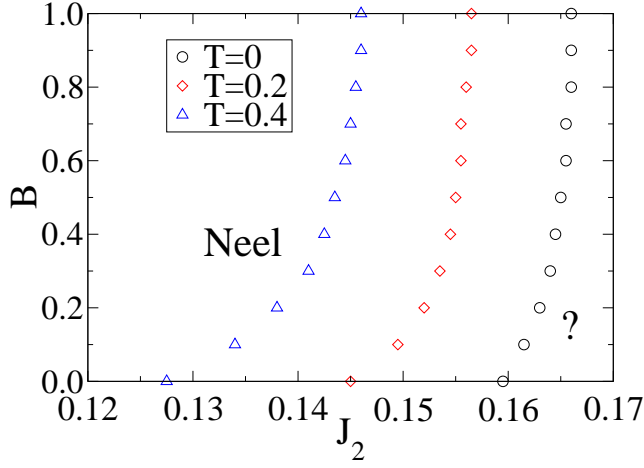


FIG. S1: Melting of Néel order for  $S=3/2$  in the  $B$ - $J_2$  plane for  $T = 0, 0.2, 0.4$  (in units of  $J_1$ ). To the left of the curve, there is stable canted Néel order. To the right, fluctuations melt the in-plane Néel order.

The matrix  $P$  preserves the commutation relations of the bosonic operators and diagonalizes the Hamiltonian, giving  $P^\dagger H P = \text{Diag}\{\Omega_{\mathbf{k}}^-, \Omega_{\mathbf{k}}^+, \Omega_{\mathbf{k}}^-, \Omega_{\mathbf{k}}^+\}$ .

The expectation value of spin moments can be calcu-

lated in terms of this new basis. For example, the in-plane component of the spin is given by

$$\frac{1}{N} \sum_i \langle S_{i,\alpha=1}^x \rangle = (S + 1/2) \cos \chi - \frac{\cos \chi}{2N} \times \sum_{\mathbf{k} > 0} [\cos 2\theta \{1 + 2n_B(\Omega_{\mathbf{k},-})\} + \cos 2\phi \{1 + 2n_B(\Omega_{\mathbf{k},+})\}], \quad (\text{S11})$$

where  $n_B(\cdot)$  denotes the Bose distribution function. For  $T \neq 0$ , a small coupling along the third dimension is necessary to allow for a stable magnetically ordered state. We take this into account by imposing an infrared cutoff  $\Lambda$  which is of the order the interplane coupling; modes with energy greater than  $\Lambda$  look like 2d spin waves.

As  $J_2$  is increased, fluctuations around the Néel state increase. We expect the Néel state to melt when fluctuations become comparable to the magnitude of the ordered moment. As discussed in the main body, we choose our melting criterion to  $\sqrt{\langle S_x^2 \rangle - \langle S_x \rangle^2} = 3\langle S_x \rangle$ , which gives a critical  $J_2/J_1$  in agreement with recent variational Monte Carlo results for  $S = 1/2$ . The resulting melting curve for  $S = 3/2$ , at zero temperature and at small temperatures, is shown in Fig.S1.